Surface Science 716 (2022) 121954

Contents lists available at ScienceDirect

Surface Science

journal homepage: www.elsevier.com/locate/susc

Role of facet in the competitive pathway of ethylene epoxidation

Aathira Nair [a], Nivedita Kenge [a], Kavita Joshi [*,a,b]

[a] Physical and Materials Chemistry Division, CSIR-National Chemical Laboratory, Dr. Homi Bhabha Road, Pune 411008, India
[b] Academy of Scientific and Innovative Research (AcSIR), Ghaziabad 201002, India

ARTICLE INFO

Keywords:
DFT
Epoxidation
Ethylene Oxide (EtO)
OMC
Ag(100)
Ag(111)

ABSTRACT

Ethylene epoxide (EtO) is used as raw material for a broad range of products from pharmaceuticals and plastics to paints and adhesives. Although the reaction of ethylene interacting with preadsorbed oxygen on Ag surface is known for decades, the underlying mechanism of EtO formation is not completely understood. Successful investigation of oxametallacycle (OMC) intermediate common to selective as well as non-selective pathways has ensured at least 50% selectivity. The current study brings out the electronic signatures of distinct conformers of OMC stabilised on two different facets of Ag viz. (100) and (111). There are subtle differences between OMC conformers observed on these two facets with near-eclipsed on Ag(100) and near-staggered on Ag(111). A detailed analysis of Ag-O, C-O, C-C, and Ag-C interactions along with projected Density of States (pDOS) and projected Crystal Orbital Hamilton Population (pCOHP) imply towards ring closure on Ag(100) and hydrogen transfer on Ag(111). Finally, our understanding based on electronic and structural signatures are backed up by activation barriers computed through NEB calculations. Activation barrier for EtO is lower on (100) as compared to (111) facet. Thus, our study sheds light on how these differences between OMC affect the selectivity towards EtO.

1. Introduction

Ethylene oxide is widely used as a raw material to produce some of the industrially important derivatives such as ethylene glycol, ethoxylates, ethanolamines, glycol ethers, polyethylene glycol, etc. The global market for ethylene oxide is estimated to grow by 3% from 2021 to 2026 [1]. Therefore, even modest improvements in the epoxidation mechanism will significantly benefit the economy. While intense efforts have been made for decades there are still ambiguities in finer details of underlying mechanism of epoxidation. Involvement of electrophilic oxygen and effect of oxygen coverage has been the focal point of research in the past few decades[2–14]. Direct epoxidation and intermediate formation (OMC) are two pathways suggested for EtO formation[15–18]. Although not completely understood, theoretical studies point out direct epoxidation to be 100% selective. On the flip side, formation of OMC explains 50% selectivity towards EtO[9]. Thus, selectivity greater than 80% achieved at industrial scale is to be perceived comprehensively. Hence, role of various factors like use of promoters,[19,20] polycrystalline facets of Ag,[21–24] and presence of subsurface oxygen[25] are under investigation. Since the discovery of OMC[17] and it's fundamental role in selective and non-selective ethylene oxidation,[16] immense volume of work has been carried out with an aim to understand the principles behind selectivity and then improving it further in favour of EtO formation [16,20,26–31]. Thermodynamically the most stable facet is Ag(111) which has 50% selectivity without promoters[32]. However, studies elevate Ag(100) as a promising facet for EtO selectivity [33,34]. Of facets with lower Miller indices, Ag(100) flaunts high selectivity of 75% [22]. Comparative studies on Ag facets with lower miller indices using DFT and Monte Carlo simulations also points Ag (100) facet to favour EtO formation even under industrial temperature conditions (500-600K)[23]. On the other hand, Ag(111) predominates in the commercially available polycrystalline catalyst in presence of embedded promoters. This difference of selectivity between two silver facets have developed considerable interest especially in past two decades. Formation of OMC is an important step in epoxidation and various studies have been carried out to get deeper insights of it. Linic and Barteau studied OMC formation on Ag clusters and differentiated them based on coordination of oxygen with Ag. They observed that OMC with oxygen connected to two Ag atoms undergoes ring closure[28]. Kokalj *et.al.* demonstrated with the help of DFT studies that Ag(100) facet has lower energy barrier for the formation of oxametallacycle intermediate wrt to the step facet [35]. Bocquet *et. al.* highlighted the role

* Corresponding author.
E-mail addresses: a.nair@ncl.res.in (A. Nair), k.joshi@ncl.res.in (K. Joshi).

https://doi.org/10.1016/j.susc.2021.121954
Received 14 July 2021; Received in revised form 12 September 2021; Accepted 25 September 2021
Available online 30 September 2021

of the stoichiometric composition of oxygen adsorbed on Ag(111) surface which facilitate the cyclisation of OMC for the formation of EtO [36]. Christopher et. al. was successful to demonstrate high EtO selectivity for silver nanowire which has maximum Ag(100) and modest amount of Ag(111) concentration [22]. The study on the effect of OMC orientation towards selectivity claims syn (eclipsed) arrangement to favour ring closure while anti(staggered) arrangement hinders selectivity by facilitating H migration [37]. Thus, role of facet for tuning the interactions in the selection process lies fundamental to EtO selectivity. To summarize, 1,2-H shift is integral to non-selective pathway whereas strengthening of C-H bond, and preservation of ethylene symmetry are crucially important to achieve highest possible selectivity towards EtO. In the present work, we demonstrate role of facet in determining the selectivity by investigating the similarities and differences in the OMC formed on these two facets. To connect structural observations with that of underlying electronic structure, we have examined Ag-O, Ag-C, Ag-Ag, C-O and C-H interactions with pDOS and pCOHP.

2. Computational Details

All the calculations are carried out within the Kohn-Sham formalism of Density Functional Theory (DFT). Projector Augmented Wave potential[38,39] is used, with Perdew Burke Ehrzenhof (PBE)[40] approximation for the exchange-correlation and generalized gradient approximation,[41] as implemented in planewave, pseudopotential based code, Vienna Ab initio Simulation Package (*VASP*).[42–44] The lattice parameter computed for Ag [4.10 Å] within the framework is within 1% of experimentally measured lattice parameter [4.09 Å]. Van der Waals corrections are applied to account dynamic correlations between fluctuating charge distribution by selecting Grimme method (DFT-D2).[45] Two different facets of Ag, (100) and (111) are modeled as slabs by cleaving a surface with 4 layers in 100 (111) direction with ASE keeping the bottom layer fixed[46]. Thus, the supercell used is 3x3x4 for both facets. We have also tested that the trends remain unchanged even if we model the slab as 4x4x4 or 3x3x5, i.e. either by choosing a larger supercell or increasing the number of layers. 20 Å of vacuum along z-axis which is also adjusted as 100 (111) direction of the crystal is found sufficient to avoid interaction between adjacent images of planes along the z-direction. Geometry optimization is carried out with a force cutoff of 0.01 eV/Å on the unfixed atoms and the total energies are converged below 10^{-4} eV for each SCF cycle. A Monkhorst-Pack grid of 6x6x1 is used for (100) and that of 5x5x1 for (111) facet. To compute the pDOS, Löwdin charges on individual atoms, and COHP, LOBSTER package is employed.[47–50] We have also confirmed that calculating pDOS using higher k-points does not change our results. Adsorption energy (E_{ads}) and Energy of formation (E_f) are calculated according to formulae as below,

$E_{ads} = E_{Ag-O}$ - ($E_{slab} + E_O$) where E_{Ag-O} is the energy of the surface with adsorbed oxygen, E_{slab} is the energy of the bare surface and E_O is the energy of the atomic oxygen. We note that, although atomic oxygen is taken as reference for computing adsorption energies, with molecular oxygen as a reference state, the difference in adsorption energies is of the order of 1 meV.

$E_f = E_{OMC}$ - ($E_{Ag-O} + E_{Et}$) where E_{OMC} is the energy of the surface with OMC, E_{Ag-O} is the energy of the surface with adsorbed oxygen, and E_{Et} is the energy of the Ethylene molecule. Nudged eElastic bBand (NEB) is used to find the minimum energy path between reactant and product. We have used CI-NEB (climbing image nudged elastic band) to determine the energy barrier on both facets towards EtO formation. A force cut off of 0.1 eV/Å and spring constant of -5 is employed in the calculation.

3. Results and Discussion

In this section, we take a look at finer details regarding electronic structure of OMC, on two facets of Ag, (100) and (111). Atomic oxygen is adsorbed at distinct adsorption sites of these two facets. Oxygen was placed at 1-fold top (1FT), 2-fold bridge (2FB), and 4-fold hollow (4FH) on Ag(100) surface. On Ag(111) surface apart from 1FT, 2FB, oxygen was also placed at 3-fold fcc hollow (3FH-1), and 3-fold hcp hollow (3FH-2). Optimization resulted in oxygen placed at 2FB site to adjust in a tetra-coordinated site making it the most stable conformation among others in the case of Ag(100). However in case of Ag(111), 3FH-1 was found to be the most stable adsorption site for O. It is observed that higher the coordination of oxygen, greater is its tendency to acquire charge. Löwdin charge of tetra-coordinated oxygen on Ag(100) is slightly more (-0.93 e^-) than tri-coordinated oxygen on Ag(111) (-0.89 e^-). Even in the presence of differently coordinated oxygen on the facets, the average charge on surface for both the facets remains comparable. Interestingly adsorption energy of oxygen (E_{ads}) on Ag(100) is -5.95 eV whereas it is -5.41 eV on Ag(111) indicating that oxygen adsorption is more favoured on Ag(100) than Ag(111). Further, all Ag-O bond-lengths are 2.25 Å on Ag(100) whereas they are 2.13 Å in case of Ag(111) suggesting that Ag-O bonds are weaker on Ag(100) as compared to those on Ag(111). It is fascinating to note that Ag(100) facet undergoes reconstruction upon adsorption of oxygen leaving traces of Ag(111) on the surface. In contrast no such sign of surface reconstruction is visible on Ag(111). Further, the configuration on (100) attains lower symmetry than that on (111).

OMC is a common intermediate for two pathways of epoxidation viz., selective and non selective. It is described as a cyclic structure consisting of one of the carbons (C1) of ethylene connected to the preadsorbed oxygen on Ag surface and another carbon (C2) of Et connected to the surface Ag. Ethylene was adsorbed on Ag-O complex in various orientations to scan different conformers of OMC. Energetically most favoured OMCs formed on these two facets are shown in Fig. 1. As can be seen from the figure, there are subtle differences in the OMC conformers formed on these two facets.

In Table 1 we have noted formation energies, Ag-O, C-O, and all C-H bond-lengths along with dihedral angles for both OMCs. Oxygen was tetra-coordinated on Ag(100) which is now tri-coordinated when OMC is formed. Same is the case with Ag(111) in which oxygen coordination changed from 3 to 2 upon formation of OMC. Despite of all Ag-O bond-lengths being identical before co-adsorption of ethylene on both the facets, formation of OMC leads to weaker bonds with uneven Ag-O bond-lengths. These elongated bonds can facilitate release of oxygen from the surface once the product is formed. However when Ag-O bonds of OMCs formed on Ag(100) and Ag(111) are compared (refer Tab. 1), the later are relatively stronger. Though C(1)-C(2) bond-lengths are same for both the facets (1.51Å), C(1)-O bond of OMC@100 is longer than OMC@111. Dihedral angles for OMC@100 are 2.2^o and 5.7^o. The value of dihedral angle is slightly away from 0^o and hence it is referred as near-eclipsed conformation. On the other hand, dihedral angles of OMC@111 are 33.6^o and 41.7^o hence, referred as near-staggered configuration. The difference in conformations is also pointed out from the charges on individual atoms as shown in Fig. 2. From the distribution of charges on hydrogen atoms attached to C(1) and C(2), we note that OMC@100 has two pairs of hydrogen atoms having same environment as should be in the case of near eclipsed structure. On the contrary, for OMC@111, all four hydrogen atoms have different magnitude of charges which indicates that all of them experience different environment like in the case of a near staggered conformation. To summarize, relatively strong Ag-O bond, unequal strength of C-H bonds with one of them relatively elongated along with the near staggered conformation of OMC@111 provides a locale for hydrogen transfer. On the other hand, near-eclipsed conformer emphasizes the hindrance to hydrogen transfer and maintains the symmetry of both carbons of OMC@100. So far, we have investigated structural differences in the OMCs formed on two different facets. Further, we analyse the electronic structure of these two OMCs with the help of site specific pDOS and pCOHP. Fig. 3 brings out the variation in the electronic structure of Ag atoms from (100) and (111)

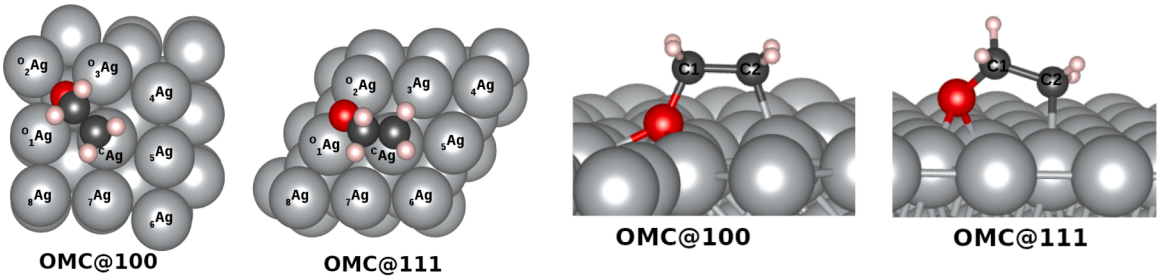

(a) Top view of OMC structure (b) side view of OMC structures

Fig. 1. (a)Top and (b) side views of OMC@100 and OMC@111 are shown. Subtle difference in the structure of these two OMCs is evident from side view.

Table 1
Formation energies (E_f), bond-lengths, and dihedral angles of OMC@100 and OMC@111 are tabulated.

System	E_f(eV)	Bond lengths (Å)						Dihedral Angle
		Ag-O	C(1)-O	C(1)-H(3)	C(1)-H(4)	C(2)-H(1)	C(2)-H(2)	
OMC@100	-0.81	2.25, 2.32, 2.36	1.46	1.105	1.106	1.097	1.097	2.2°, 5.7°
OMC@111	-1.12	2.24, 2.25	1.43	1.112	1.106	1.100	1.098	33.8°, 41.7°

Fig. 2. Configurations of most stable OMC on Ag(100) and Ag(111) along with Löwdin charges. The charge variation on H atoms bring out subtle difference in OMCs formed on these two facets.

facets upon oxygen adsorption. Structural rearrangements observed in case of Ag(100) upon oxygen adsorption were also reflected in their pDOS. In Fig. 3, we represent pDOS of Ag atoms which were coordinated with adsorbed oxygen for both facets (100) (Fig. 3-a,b) and (111) (Fig. 3-c,d). The comparison is made between Ag-5s (Fig. 3 a and c) and Ag-4d (Fig. 3 b and d) states of two facets. In absence of adsorbed oxygen, all atoms on the surface are equivalent and exhibit identical pDOS, tagged as "bare" in the plots. In case of Ag (100), since adsorbed oxygen is coordinated with 4 Ag atoms, pDOS for those 4 Ag atoms is shown. In case of Ag (111), since oxygen is coordinated with three Ag atoms, their pDOS is shown along with "bare" Ag (111). The difference in both these cases is evident. Since, upon oxygen adsorption there is hardly any surface rearrangements in case of Ag (111), the pDOS for all the coordinated Ag atoms are almost similar (see Fig. 3 c and d). Although, they differ from the case of pDOS for "bare" Ag atoms. Contrary to this, Ag (100) undergoes (partial) surface reconstruction and hence Ag atoms which were equivalent before oxygen adsorption, are no longer equivalent. The change in their connectivity with the surrounding atoms (Ag as well as oxygen) is reflected in their pDOS. The variation is more evident if we compare it with that of Ag(111). All three Ag atoms (coordinated with oxygen) in case of Ag (111), have pDOS overlapping on each other, whereas, every atom coordinated with oxygen in case of Ag (100) show a distinct pDOS. Thus, pDOS for Ag-4d in case of Ag(111) show only two curves, one for Ag coordinated with O and another for non-coordinated Ag atoms. On the contrary, pDOS of Ag-4d for Ag (100) atoms show distinct lines for each of the Ag atom coordinated with oxygen. The rearrangement of atoms upon oxygen adsorption in case of Ag (100) is also shown in the inset of Fig. 3 (b) and is compared with that of Ag (111) (shown in the inset of Fig. 3 (d)). Although, Ag (100) does not get restructured completely into Ag (111), upon oxygen adsorption, glimpses of Ag(111) are seen in the restructured Ag(100) and are highlighted to aid the observer. Further, in comparison to bare surface the intensity of Ag-5s peaks has decreased for both Ag-O(100) and Ag-O (111) complexes. This decrease of intensity can be understood as loss of charge by surface Ag atoms to adsorbed oxygen. It is also confirmed from Löwdin charges calculated on both, Ag atoms and oxygen. This variation of intensity is however not evident for Ag-4d states. Hence, Ag-5s states dominate in interaction with oxygen than Ag-4d states.

Fig. 4 brings out an interesting observation regarding pDOS of hydrogen atoms in OMCs formed on Ag(100) and Ag(111). Based on the structural analysis, we propose that the hydrogen atoms connected to same carbon atom in an OMC@100 are equivalent, in terms of their bonding as well as underlying electronic structure. PDOS of four hydrogen atoms in OMC@100 is shown in Fig. 4 (a) which show two distinct lines indicating two types of hydrogen atoms, connected to two different carbon atoms. Since the carbon atoms within OMC experience different environment (one is connected to oxygen whereas other is connected to surface Ag atom) the hydrogen atoms connected to these two carbon atoms also show slight variance in their pDOS reflecting the variation in their connectivity. On the other hand, hydrogen atoms in OMC@111 are all distinct in terms of their C-H bond lengths and environment which also reflects into their pDOS plots. This is in line

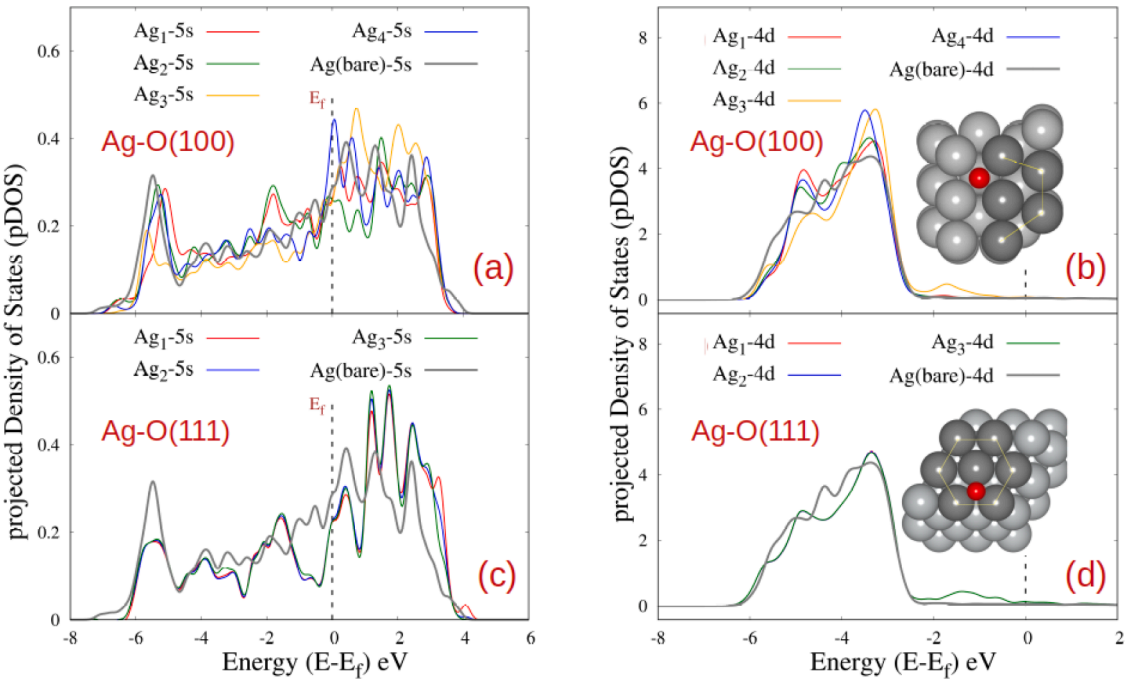

Fig. 3. Figures (a) and (b) compares site specific pDOS for Ag-5s and Ag-4d states respectively of oxygen adsorbed Ag(100) surface with that of bare Ag(100) surface. Figures (c) and (d) shows the comparison of Ag-5s and Ag-4d states respectively of oxygen adsorbed Ag(111) surface with that of bare Ag(111) surface. The scattered distribution of pDOS in Ag-O(100) indicate reconstruction of the surface which is absent for Ag-O(111).

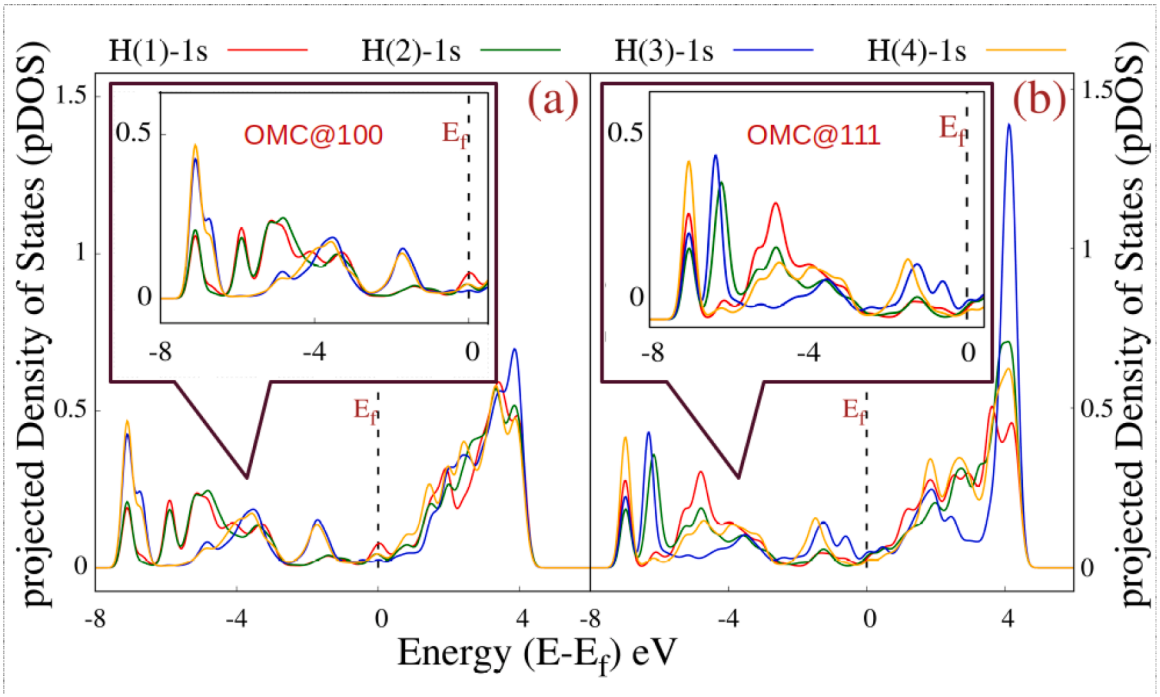

Fig. 4. pDOS of H-1s for (a) OMC@100 and (b) OMC@111 conformers. In case of OMC@100, hydrogen atoms connected to one carbon have identical pDOS, thus resulting into two pairs. In case of OMC@111, all the hydrogen atoms are distinguishable as evident from their pDOS. Region below Fermi level is magnified and shown in the inset.

with observation made from dihedral angle and Löwdin charges on H atoms of both facets which distinguishes OMC@100 and OMC@111 as near eclipsed and near staggered respectively. pDOS represents the density of states specific to an atom. To get a complete picture of the interaction between various atoms of the complex, we have analysed COHP for various pairs of atoms like C1-O, C2-O, Ag-O, etc. In simpler words, COHP is a theoretical bond-detecting tool for solids. It is a "bond-weighted" density-of-states between a pair of adjacent

atoms. Integration of COHP curves leads to bond-strength. In COHP, bonding and anti-bonding interactions are represented by negative and positive values respectively [51]. We investigate C1-O, C2-O, and Ag-O interactions in order to understand the differences in OMC@100 and

OMC@111 conformers. COHP plots for C1-O and C2-O are shown in Fig. 5- a and b respectively. Comparing the magnitude of COHP of C1-O interaction with that of C2-O clearly shows that C2-O interactions are much weaker as observed in Fig. 5. It is also observed that C1-O interaction peaks for OMC@111 have slightly shifted towards Fermi level in comparison to that of OMC@100. The strength of interaction can be validated from IpCOHP values, -6.96 eV for OMC@100 and -7.41 eV for OMC@111. However, even if the C2-O interactions in both cases seem comparable, there are subtle differences. In case of OMC@100, contribution from bonding molecular orbitals (BMO) is sharper whereas the peak near Fermi, indicating contribution from anti-bonding molecular orbitals is sharper for OMC@111. Further, when COHP for Ag-O interactions are compared for OMC@100 and OMC@111, it can be seen that Ag-O interaction is weaker in case of OMC@100 as can be seen from Fig. 6. IpCOHP values of 2 elongated Ag-O bonds out of 3 are -0.51 eV and -0.56 eV for OMC@100 and -0.73 eV, -0.75 eV for OMC@111. This confirms the weakening of Ag-O bonds on OMC@100.

So far, we have held our attention on structural and electronic data for OMC formed on Ag(100) and Ag(111) from which we noted how OMC intermediates are subtly different for both the facets. Weaker Ag-O bonds, reconstructed surface due to oxygen adsorption on facet, dihedral angles of OMC establishing near eclipsed structure and weak C1-O interactions are noteworthy observations made for OMC@100. Similarly OMC@111 has comparatively shorter or stronger Ag-O bonds than OMC@100. Near staggered configuration along with comparatively strong C1-O interactions are also emphasised in our investigation.

By assembling all the above discussed factors together, it is found that OMC@100 favours EtO formation over OMC@111. To support this, Wwe have employed CI-NEB to determine the energy barrier on both facets towards EtO formation. The result shows that the transition state energy barrier for OMC@111 towards formation of EtO is slightly higher than OMC@100 as shown in Fig. 7. We note that the difference in activation barrier between the two is 0.0517 eV. Agreeably the difference in the activation barrier is marginal. However, our observations based on structure, bond-lengths, dihedral angle, charges, pDOS, and pCOHP suggest OMC@100 to favour EtO formation and OMC@111 provides a locale for hydrogen transfer. NEB results have added an extra evidence to the above noted factors. We also noticed that upon EtO formation Ag-O interaction reduces significantly for both the facets which can aid in easy abstraction of product.

4. Conclusions

We investigated the role of facet in epoxidation by comparing

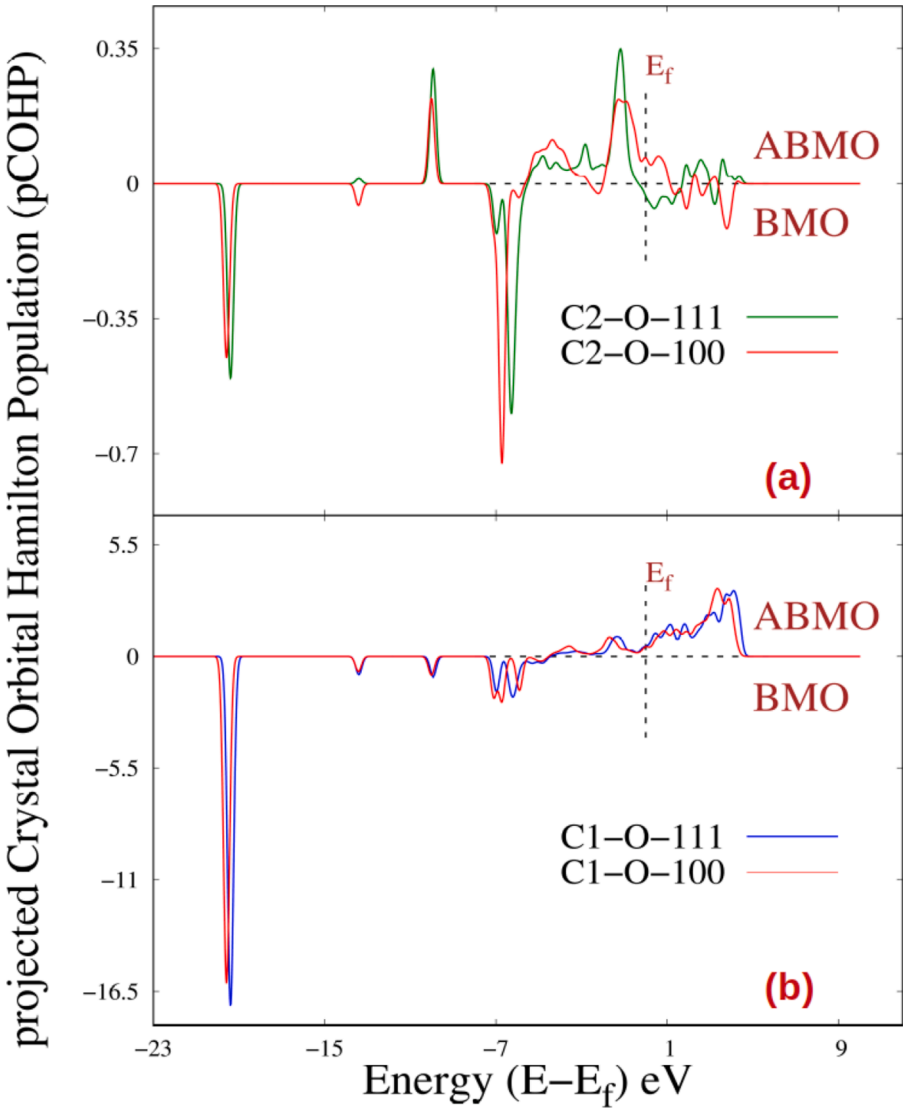

Fig. 5. Figure (a) represents weak long range C2-O interactions for OMC@100 (C2-O-100) and OMC@111(C2-O-111). Figure (b) compares C1-O interactions for OMC@100 (C1-O-100) and OMC@111 (C1-O-111). C1-O interactions are found to be slightly weaker for OMC@100 which is favourable for EtO formation.

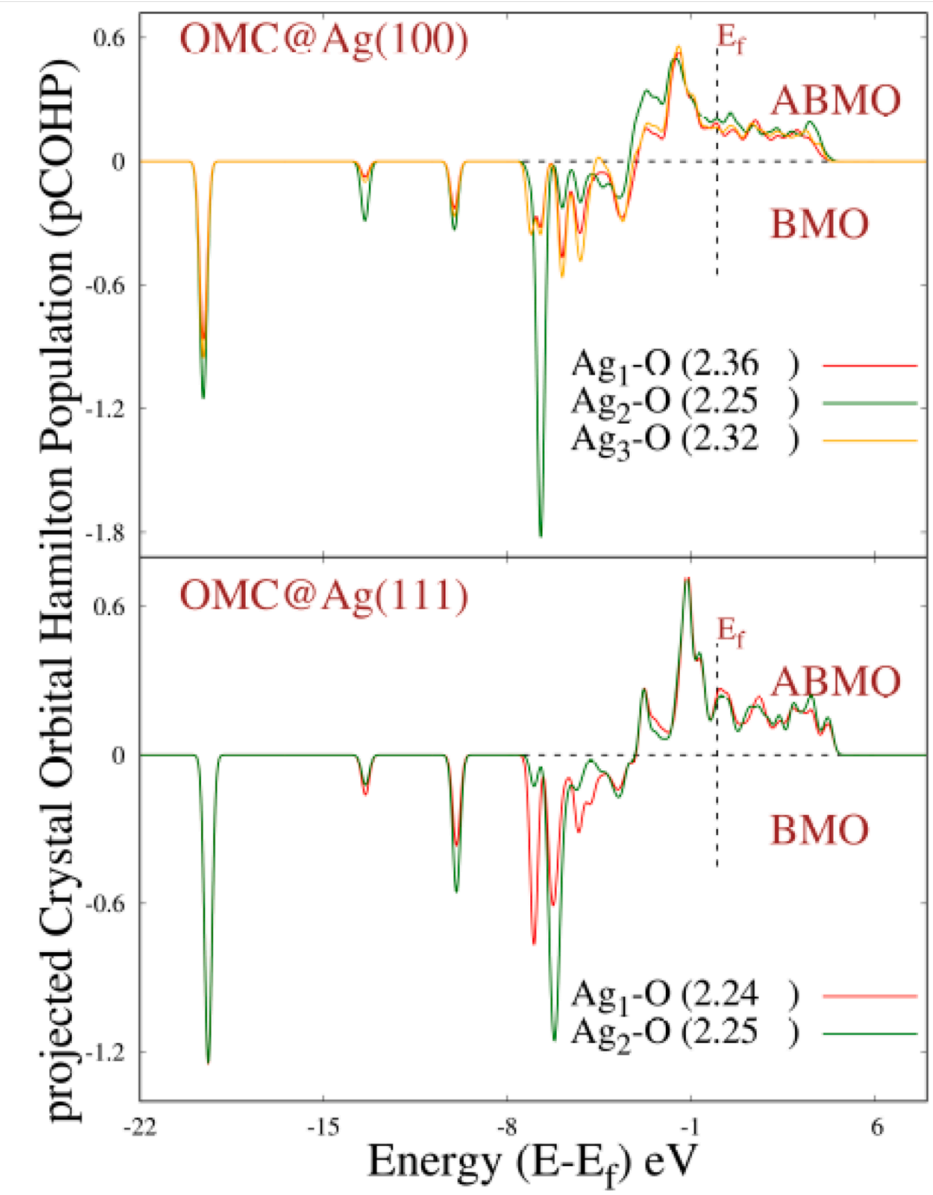

Fig. 6. Ag-O interactions for OMC@100 (above) and OMC@111 (below) are compared. OMC@100 has weaker interactions which can help facilitate release of product formed on surface.

industrially important Ag(111) facet with Ag(100) facet. It was interesting to note that Ag(100) undergoes reconstruction on oxygen adsorption and has traces of Ag(111) facet on the distorted surface. However presence of oxygen does not have much effect on Ag(111) facet. Oxygen adsorption is favoured on distorted Ag(100) over Ag(111) facet. OMC which acts as intermediate for both epoxide and acetaldehyde formation is unique for both the facets and is distinguished with the help of bondlength analysis, dihedral angles, Löwdin charges, site specific pDOS, and pCOHP data analysis. OMC@100 orients in a near eclipsed fashion while OMC@111 takes a near staggered configuration. This is supported by Löwdin charges as well as site specific pDOS for H-1s states of hydrogen atoms attached to carbons on OMCs. By digging deeper through our observations it was deduced that weak C1-O interactions along with near eclipsed orientation and shorter C2-O bond distance for OMC@100, ring closure is favoured leading to EtO formation. Weak Ag-O bonds can aid to selectivity by easing the release of product formed on surface. For OMC@111 however, comparatively stronger C1-O interactions, near staggered orientation, shorter Ag-O bonds and slight elongation of one of the C-H bonds can cause hindrance to selectivity. Thus, we can draw inference that OMC@100 favours EtO formation than OMC@111. CI-NEB supports the above observation as the results clearly showed that the energy barrier for EtO formation from OMC@111 is higher than that for OMC@100. This makes Ag(100) facet comparatively facile for EtO formation than Ag (111) facet. Our study finds that oxygen adsorption is favoured on Ag (100) while OMC stabilizes better on Ag(111) facet. Further, the activation barrier towards EtO formation from OMC formed on Ag(100) is lower in comparison to OMC on Ag(111). Therefore facet determination is a complex matter of contention and it is significant to consider the interplay of various factors for deciding the suitable facet for epoxidation.

CRediT authorship contribution statement

Aathira Nair: Formal analysis, Writing – original draft, Writing – review & editing. **Nivedita Kenge:** Conceptualization, Methodology, Writing – original draft. **Kavita Joshi:** Conceptualization, Supervision, Project administration, Funding acquisition.

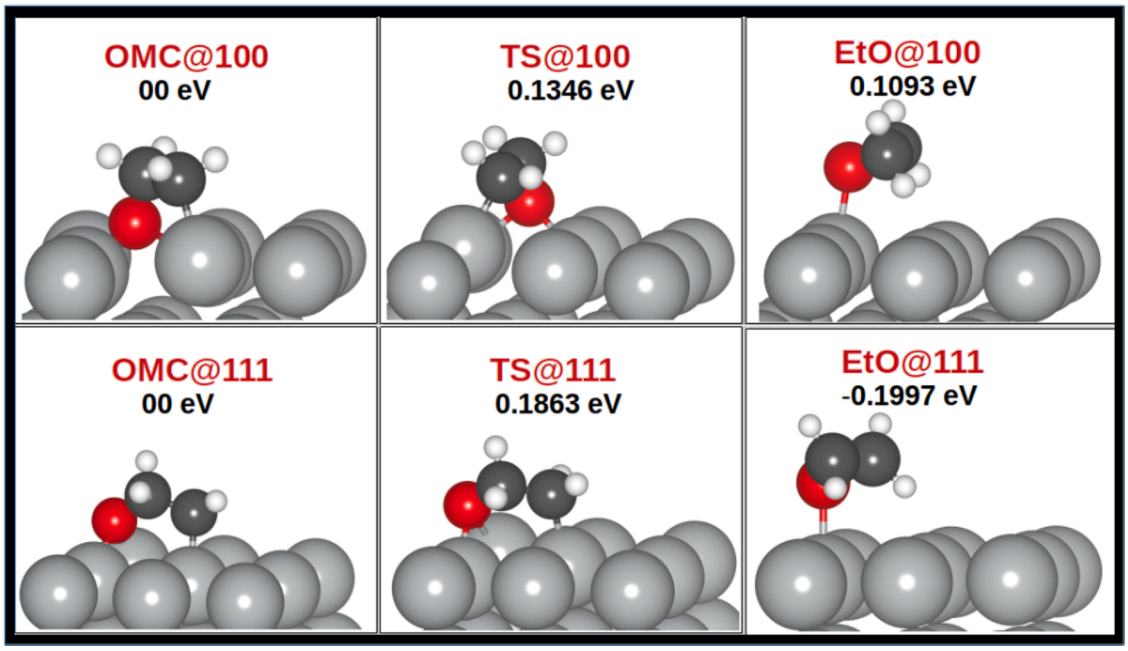

Fig. 7. Comparison of transition state energy barrier for formation of EtO product from OMC@100 and OMC@111.

Declaration of Competing Interest

This manuscript has not been submitted to, nor is under review at, another journal or other publishing venue.

Acknowledgment

Authors thank CSIR-4PI for the computational facility and MLP100526 for financial support.

References

[1] Ethylene oxide market - growth, trends, covid-19 impact, and forecasts (2021 - 2026), https://www.mordorintelligence.com/industry-reports/ethylene-oxide-market.
[2] X. Bao, M. Muhler, T. Schedel-Niedrig, R. Schlögl, Phys. Rev. B 54 (1996) 2249–2262, https://doi.org/10.1103/PhysRevB.54.2249.
[3] V.I. Avdeev, A.I. Boronin, S.V. Koscheev, G.M. Zhidomirov, Journal of Molecular Catalysis A: Chemical 154 (1) (2000) 257–270, https://doi.org/10.1016/S1381-1169(99)00395-7.
[4] V.I. Bukhtiyarov, V.V. Kaichev, Journal of Molecular Catalysis A: Chemical 158 (1) (2000) 167–172, https://doi.org/10.1016/S1381-1169(00)00062-5.
[5] W.-X. Li, C. Stampfl, M. Scheffler, Phys. Rev. B 65 (2002) 075407, https://doi.org/10.1103/PhysRevB.65.075407.
[6] V.V. Kaichev, V.I. Bukhtiyarov, M. Hävecker, A. Knop-Gercke, R.W. Mayer, R. Schlögl, Kinetics and Catalysis 44 (3) (2003) 432–440, https://doi.org/10.1023/A:1024459305551.
[7] J. Schnadt, J. Knudsen, X.L. Hu, A. Michaelides, R.T. Vang, K. Reuter, Z. Li, E. Lægsgaard, M. Scheffler, F. Besenbacher, Physical Review B 80 (7) (2009), https://doi.org/10.1103/PhysRevB.80.075424.
[8] M.F. Fellah, R.A. van Santen, I. Onal, Catalysis Letters 141 (6) (2011) 762–771, https://doi.org/10.1007/s10562-011-0614-2.
[9] M.O. Ozbek, I. Onal, R.A. van Santen, Topics in Catalysis (2012) 710–717, https://doi.org/10.1007/s11244-012-9870-7.
[10] T.C.R. Rocha, A. Oestereich, D.V. Demidov, M. Hävecker, S. Zafeiratos, G. Weinberg, V.I. Bukhtiyarov, A. Knop-Gericke, R. Schlögl, Physical Chemistry Chemical Physics 14 (13) (2012) 4554, https://doi.org/10.1039/c2cp22472k.
[11] S. Böcklein, S. Günther, J. Wintterlin, Angewandte Chemie International Edition 52 (21) (2013) 5518–5521, https://doi.org/10.1002/anie.201210209.
[12] N.M. Martin, S. Klacar, H. Grönbeck, J. Knudsen, J. Schnadt, S. Blomberg, J. Gustafson, E. Lundgren, The Journal of Physical Chemistry C 118 (28) (2014) 15324–15331, https://doi.org/10.1021/jp504387p.
[13] T.E. Jones, T.C.R. Rocha, A. Knop-Gericke, C. Stampfl, R. Schlögl, S. Piccinin, ACS Catalysis 5 (10) (2015) 5846–5850, https://doi.org/10.1021/acscatal.5b01543.
[14] N. Kenge, S. Pitale, K. Joshi, Surface Science 679 (2019) 188–195, https://doi.org/10.1016/j.susc.2018.09.009.https://www.sciencedirect.com/science/article/pii/S0039602818306848
[15] G.H. Twigg, Trans. Faraday Soc. 42 (1946) 284–290, https://doi.org/10.1039/TF9464200284.
[16] E.L. Force, A.T. Bell, Journal of Catalysis 40 (3) (1975) 356–371, https://doi.org/10.1016/0021-9517(75)90267-5.
[17] L. Suljo, A. Barteau Mark, Journal of the American Chemical Society 124 (2) (2002) 310–317, https://doi.org/10.1021/ja0118136.
[18] M.O. Özbek, R.A. van Santen, Catalysis Letters 143 (2) (2013) 131–141, https://doi.org/10.1007/s10562-012-0957-3.
[19] M.O. Ozbek, I. Onal, R.A. Van Santen, Journal of Physics: Condensed Matter 23 (40) (2011) 404202, https://doi.org/10.1088/0953-8984/23/40/404202.
[20] S. Linic, M.A. Barteau, Journal of the American Chemical Society 126 (26) (2004) 8086–8087, https://doi.org/10.1021/ja048462q.
[21] A. Kokalj, P. Gava, S. de Gironcoli, S. Baroni, The Journal of Physical Chemistry C 112 (4) (2008) 1019–1027, https://doi.org/10.1021/jp0747961.
[22] P. Christopher, S. Linic, ChemCatChem 2 (1) (2010) 78–83, https://doi.org/10.1002/cctc.200900231.
[23] M. Huš, A. Hellman, ACS Catalysis 9 (2) (2019) 1183–1196, https://doi.org/10.1021/acscatal.8b04512.
[24] L. Zhu, W. Zhang, J. Zhu, D. Cheng, Applied Catalysis A: General 538 (2017) 27–36, https://doi.org/10.1016/j.apcata.2017.03.011.https://www.sciencedirect.com/science/article/pii/S0926860X17301102
[25] J. Greeley, M. Mavrikakis, The Journal of Physical Chemistry C 111 (22) (2007) 7992–7999, https://doi.org/10.1021/jp070490i.
[26] S. Linic, M.A. Barteau, Journal of Catalysis 214 (2) (2003) 200–212, https://doi.org/10.1016/S0021-9517(02)00156-2.
[27] S. Linic, M.A. Barteau, Journal of the American Chemical Society 124 (2) (2002) 310–317, https://doi.org/10.1021/ja0118136.
[28] S. Linic, M.A. Barteau, Journal of the American Chemical Society 125 (14) (2003) 4034–4035, https://doi.org/10.1021/ja029076g.PMID: 12670209
[29] J. Couves, M. Atkins, M. Hague, B.H. Sakakini, K.C. Waugh, Catalysis Letters 99 (1) (2005), https://doi.org/10.1007/s10562-004-0775-3.
[30] R.B. Grant, R.M. Lambert, Journal of Catalysis 92 (2) (1985) 364–375, https://doi.org/10.1016/0021-9517(85)90270-2.
[31] R.A. Van Santen, H.P.C.E. Kuipers, The mechanism of ethylene epoxidation 35, Academic Press, 1987, pp. 265–321, https://doi.org/10.1016/S0360-0564(08)60095-4.
[32] W.M.H. Sachtler, C. Backx, R.A. Van Santen, Catalysis Reviews 23 (1-2) (1981) 127–149, https://doi.org/10.1080/03602458108068072.
[33] P. Christopher, S. Linic, Journal of the American Chemical Society 130 (34) (2008) 11264–11265, https://doi.org/10.1021/ja803818k.PMID: 18665594
[34] A. Kokalj, P. Gava, S. de Gironcoli, S. Baroni, The Journal of Physical Chemistry C 112 (4) (2008) 1019–1027, https://doi.org/10.1021/jp0747961.
[35] A. Kokalj, P. Gava, S. de Gironcoli, S. Baroni, The Journal of Physical Chemistry C 112 (4) (2008) 1019–1027, https://doi.org/10.1021/jp0747961.
[36] M.-L. Bocquet, A. Michaelides, D. Loffreda, P. Sautet, A. Alavi, D.A. King, Journal of the American Chemical Society 125 (19) (2003) 5620–5621, https://doi.org/10.1021/ja0297741.
[37] M.-L. Bocquet, D. Loffreda, Journal of the American Chemical Society 127 (49) (2005) 17207–17215, https://doi.org/10.1021/ja051397f.PMID: 16332067
[38] P.E. Blöchl, Physical Review B 50 (1994) 17953, https://doi.org/10.1103/PhysRevB.50.17953.

[39] G. Kresse, D. Joubert, Physical Review B 59 (1999) 1758, https://doi.org/10.1103/PhysRevB.59.1758.
[40] J.P. Perdew, K. Burke, M. Ernzerhof, Physical Review Letters 77 (1996) 3865, https://doi.org/10.1103/PhysRevLett.77.3865.
[41] J.P. Perdew, K. Burke, M. Ernzerhof, Physical Review Letters 78 (1997) 1396, https://doi.org/10.1103/PhysRevLett.78.1396.
[42] G. Kresse, J. Hafner, Physical Review B 49 (1994) 14251, https://doi.org/10.1103/PhysRevB.49.14251.
[43] G. Kresse, J. Furthmüller, Physical Review B 54 (1996) 11169, https://doi.org/10.1103/PhysRevB.54.11169.
[44] G. Kresse, J. Furthmüller, Computational Materials Science 6 (1) (1996) 15, https://doi.org/10.1016/0927-0256(96)00008-0.
[45] S. Grimme, Journal of Compuatational chemistry 27 (2006) 1787–1799.https://www.ncbi.nlm.nih.gov/pubmed/16955487
[46] A.H. Larsen, J.J. Mortensen, J. Blomqvist, I.E. Castelli, R. Christensen, M. Dułak, J. Friis, M.N. Groves, B. Hammer, C. Hargus, E.D. Hermes, P.C. Jennings, P. B. Jensen, J. Kermode, J.R. Kitchin, E.L. Kolsbjerg, J. Kubal, K. Kaasbjerg, S. Lysgaard, J.B. Maronsson, T. Maxson, T. Olsen, L. Pastewka, A. Peterson, C. Rostgaard, J. Schiøtz, O. Schütt, M. Strange, K.S. Thygesen, T. Vegge, L. Vilhelmsen, M. Walter, Z. Zeng, K.W. Jacobsen, Journal of Physics: Condensed Matter 29 (27) (2017) 273002.http://stacks.iop.org/0953-8984/29/i=27/a=273002
[47] R. Dronskowski, P.E. Blöchl, The Journal of Physical Chemistry 97 (33) (1993) 8617–8624.
[48] V.L. Deringer, A.L. Tchougréeff, R. Dronskowski, The Journal of Physical Chemistry A 115 (21) (2011) 5461–5466.
[49] S. Maintz, V.L. Deringer, A.L. Tchougréeff, R. Dronskowski, Journal of Computational Chemistry 34 (29) (2013) 2557–2567, https://doi.org/10.1002/jcc.23424.
[50] S. Maintz, V.L. Deringer, A.L. Tchougréeff, R. Dronskowski, Journal of Computational Chemistry 37 (11) (2016) 1030–1035, https://doi.org/10.1002/jcc.24300.
[51] S. Steinberg, R. Dronskowski, Crystals 8 (5) (2018) 225.